The Formation Mechanism and Characterization of Al-Si Master Alloys from Sodium Fluosilicate

Gamal Mohamed Attia MAHRAN [1, 2], Abdel-Nasser Mohamed OMRAN [2] *, El-Sayed Sedek ABU SEIF [1]

[1] *King Abdulaziz University, Jeddah 21589, Saudi Arabia*
[2] *Mining and Metallurgical Department, Faculty of Engineering, Al-Azhar University, Qena 83513, Egypt*

A modified Al-Si alloy containing up to 15 wt.% Si has been obtained from the reaction of sodium fluosilicate (Na_2SiF_6) with molten aluminum. This work attempted to estimate the mechanism of the reaction of Na_2SiF_6 with molten aluminum to produce Al-Si alloys. The effect of temperature, Na_2SiF_6/Al Wt ratio and reaction time on the formation of Al-Si alloy were investigated. The thermodynamic data, kinetic and rate of the reaction were studied. The results showed the possibility of the reaction between Na_2SiF_6 and molten aluminum thermodynamically, and that this reaction might be controlled chemically. The current study aims to optimize the factors that affecting the preparation of a modified Al-Si alloy from a reduction of sodium fluosilicate using molten aluminium. Temperature 950 ºC, reaction time $20-25$ min and Na_2SiF_6/Al Wt ratio related to the applied Si percentage. The prepared alloys could be modified due to the presence of Na_2SiF_6 in the used material as a source of sodium in response to modifying the produced Al-Si alloys. The microstructure by using LOM, SEM, and EDX proved that the needle-like silicon converts to fine fibrous. The volume fraction of primary Si reduces and the eutectic point moves to a higher silicon concentration. The modification improves the wear characteristics and increases the tensile and hardness.

Keywords: Al-Si alloys, sodium fluosilicate, microstructure, mechanical properties, wear.

1. INTRODUCTION

Aluminium–silicon alloys that contain Si as the main alloying element covers more than ninety percent of the total manufactured Al castings and have wide range of uses, particularly in the automotive, aerospace and engineering sectors [1]. The importance of Al-Si alloys among aluminum cast products owing to their high cast-ability, low specific gravity, low shrinkage, good weld-ability and good resistance to wear and corrosion [2]. The silicon content in the aluminium–silicon alloys ranged from $4-25$ %. Al-Si alloys are further classified as hypoeutectic (less than 12 % Si), eutectic (ranged from $12-13$ % Si) and hypereutectic (varied from $14-25$ % Si) based on the silicon concentration in the alloy [3, 4]. The mechanical properties of the aluminium–silicon alloys depend on the distribution, shape, and size of eutectic and primary silicon phases. Roundness, goodness, and homogeneity of silicon particles increase the strength of Al-Si alloys [5, 6]. By study, the mechanical and tribological properties proved to be the most important properties in several engineering industries and automobile applications as the wear and friction of components in such industries are the major problems. Many researchers have studied the abrasive and sliding wear behavior of aluminium–silicon [7]. The aluminium–silicon alloys properties depend, strongly, on the casting process, composition and melt treatment that used in the alloy. However, the commercial applications of these alloys

depend on controlling the structure of the silicon phase [8]. Silicon particles normally formed as needles enveloping dendritic matrix. The massive silicon phases cause the fracture or early crack initiation, when the components of the alloy are in tension, and they have a detrimental effect on machinability, extrudability, ductility, and strength of the alloy [9]. However, few hundreds ppm of strontium (Sr) and sodium (Na), as modifiers, can result in very fine, fibrous structure that leads to improvements in the mechanical properties [10 – 12].

Grain refiners and modifiers could be added to the molten aluminium–silicon alloys to get a combined modification and grain refinement effects. However, refining the primary silicon particles alone without modifying the eutectic silicon phase does not increase the mechanical properties [13]. Both Na and Sr are active modifiers for aluminium–silicon eutectic. It is challenging to control and keep the modification effect of Na because of fading and oxidation losses, especially at higher temperatures, and because longer holding times are necessary but Sr does not cause such problems [14, 15].

On the other hand, the phosphate ores contain fluorine in the form of calcium fluoride that used in producing phosphoric acid and super-phosphate fertilizers. The average fluorine content of these ores is about $2-4$ %. The fluorine-containing gases evolves during the production process in the form of silicon tetrafluoride (SiF_4) and hydrogen fluoride (HF), what causes air pollution problems. These gases being scrubbed by water to produce dilute fluosilicic acid. The produced fluosilicic acid could be converted into sodium fluosilicate (S.F), in the form of white crystals, by treatment with sodium chloride solution

---

* Corresponding author. Tel.: +201005405357.
E-mail address: *mranasser@hotmail.com* (A. M. Omran)

[1]. The amount of produced S.F as a by-product in superphosphate fertilizing plants was used in a small scale, such as ceramic, enamels, glass, etc. It used, as well, in producing cryolite and AlF_3 salts, and required as an electrolyte in the aluminium reduction cells, essentially for the dissolution of alumina [16, 17].

This work aims to study the parameters that affecting the reaction of Na_2SiF_6 with molten aluminium to produce Al-Si alloys, such as temperature and time, as well as, to estimate the rates of reaction at different temperatures. An attempt is made to investigate the mechanism of formation aluminium–silicon alloys through the reaction of Na_2SiF_6 with the molten aluminium.

2. EXPERIMENTAL

2.1. Materials

The used aluminium in this study is of 99.7 % purity, produced by Aluminium company of Egypt, is subjected to Elemental analysis as shown in Table 1.

Table 1. Chemical analysis in (wt.%) of aluminium before melting

Fe	Si	Cu	Mn	Mg	Ti	Na
0.03-.09	0.01	0.005	0.004	0.004	0.005	0.005

The sodium fluosilicate (Na_2SiF_6) is powdered. The chemical analysis of the used of Na_2SiF_6 is shown in Table 2.

Table 2. The chemical analysis of the used sodium fluosilicate in this study

Element, %						
F	Si	Na	Fe	S	Ti	Ca
57.54	14.02	23.72	0.001	0.001	0.0001	0.3

2.2. Procedure

The experiments were performed in a vertical tube furnace provided by mechanical stirrer having speed and temperature controllers. The aluminium (250 g) were charged into a silicon carbide crucible inside the furnace. The aluminium melt and hold at the required temperature 800 – 1000 °C. The compacted Na_2SiF_6 material, that previously prepared, was added in a suitable amount, and the crucible content was agitated using mechanical stirrer (400 rpm). After specific times (5, 10, 15, 20, 25 and 30 minutes), the crucible has been withdrawn from the furnace and the upper layer of the mixture, the slag, has been skimmed. Then the molten alloy poured into cast iron molds (30 mm diameter and 25 mm depth) and the produced alloys were chemically analyzed. Series of experiments were executed for different Na_2SiF_6 /Al ratio (*R*), reaction time (*t*) and temperature (*T*). The prepared specimens were tested; by light optical Microscopy (LOM) Olympus model BX51, electron microscopy (SEM FEI Inspect S50, Germany) attached to EDS, and XRD (model D5000) with Ni-filtered Cu-Kβ radiation (λ = 1.5408 A) Siemens made in Germany. The hardness test carried out using Brinell hardness (load 5 Kgf, 1/16 inch ball diameter according to ASTM-E10 and average 3 hardness readings were taken. The specimens for the tensile test were prepared according to ASTM-E8 for the tensile test and the

test executed by using tensile test machine. The wear rate of the produced alloys was measured using a pin-on-disk testing device at a constant load of 0.886 Kgf, at the same sliding speed of 250 rpm (4.5 m/s), the disk made of gray cast iron and the pin is represent the specimens each of them 6 mm diameter and 40 mm length.

3. RESULTS AND DISCUSION

3.1. Effect of temperature

The influence of temperature on the composition of the produced Al-Si alloys by reacting S.F with molten aluminium was studied. Other conditions are kept constant; stirring 400 rpm, time is 20 min. and S.F/Al ratio is 1. It can be seen from the Fig. 1 that the silicon percentage in the produced alloys increases by increasing the temperature from 800 to 950 °C and there was no remarkable increasing from 950 to 1000 °C and little decreasing at a temperature more than 1000 °C. The increasing from 800 to 950 °C can be due to increasing of fluidity, which leads to increasing the percentage of Si that dissolved in the bath. These results are in agreement with that obtained in the literature [18]. It is found that decreasing Si at more than 1000 °C is due to some losses of silicon content in the produced alloys might be due to oxidation. Because of the analysis of the skimmed slag which produced at 1100 °C containing Al and Si % about 1 % each more than the removed slag, which produced at 1000 °C.
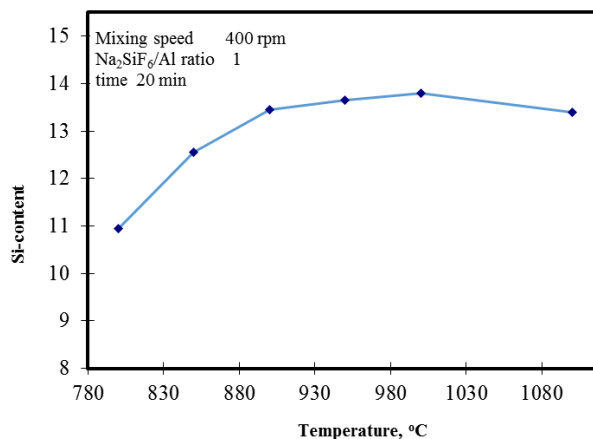

Fig. 1. Effect of temperature on the Si content in produced alloys

3.2. Effect of Na_2SiF_6 /Al ratio, *R*

Fig. 2 shows the effect of Na_2SiF_6/Al ratio (*R*) on Si contents in the produced alloys at mixing speed 400 rpm, temperature 900, and time 20 min. From the Fig. 2, it can be noticed that the Si % in the produced alloys increases linearly by increasing Na_2SiF_6/Al ratio in the range from 0.5 to 1.5 ratio, it reached up to 19 % Si at S.F/Al ratio *R* equal to 1.5. This is due to increasing the quantity of S.F in relation to the amount of molten aluminium. Imperatively, it was found, under similar conditions of the experiment, that the silicon content in the produced alloys does not reach more than 10 % on carrying out the experiments without stirring [18, 19]. In addition, the difference between the actual silicon content and theoretical silicon content increased as the *R* increases. The efficiency of the

reaction is relatively low if compared to that theoretically calculated to determine the silicon contents, as given in the following deduced equation from stiocmetry of the reaction:

$$[\%\,Si]_{Theor} = \frac{78R}{(5.22 - 0.22R)},\qquad(1)$$

where R is the Na_2SiF_6/Al wt. ratio.

The percentage of actual silicon in the produced alloy can be correlated by the empirical equation:

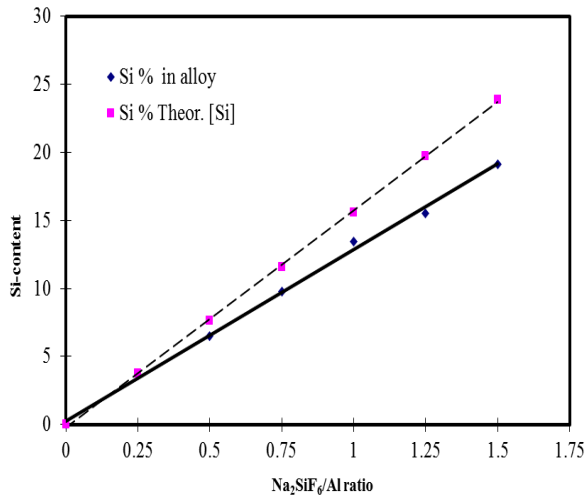$$Si\,\%\ in\ the\ alloys = 12.6\,R + 0.25,\qquad(2)$$

where: $0.5 < R < 1.5$

Fig. 2. Effect of Na_2SiF_6/Al ratio (R) on Si contents in the produced alloys

3.3. Effect of reaction time

Fig. 3 shows the relation between the Si percentage in the produced aluminium–silicon alloys and the reaction time at different temperatures 800, 850, 900, 950, and 1000. The results demonstrated that the percentage of Si in the produced alloys increases by increasing the reaction time in the range of 5 to 25 min, a further increase in the reaction time leads to a little decrease in Si percentage. Increasing the Si % contents in the produced alloys by increasing reaction time in the range of 5 to 25 min is a normal result, but it needs sufficient time to complete the reaction. The little decreases of Si for larger reaction time might be due to the increasing of products and decreasing of reactants leads to decrease the reaction rate and drive the reaction toward the equilibrium at all temperatures.

Also from Fig. 3, the silicon percentage of the produced aluminium–silicon alloys at any reaction time increased as the temperature increases at 800, 850, 900, 950 and 1000 °C. The fitting curves at these temperatures represent 5 lines in different slopes, the slop of each line represents the reaction rate K. The slopes of these lines increase by increasing the temperature. The logarithm of reaction rates $\ln K$ was plotted versus $1/T$ according to Arrhenius equation as shown in Fig. 4. From this figure, it can be shown that the experimental results give a good fitting to Arrhenius equation. The slope of the straight line was calculated to be -3257.3, from Arrhenius equation:

$$\ln K = \ln K_o - \frac{Q}{R}\left(\frac{1}{T}\right),\qquad(3)$$

where K is the reaction rate; T is the temperature in Kelven degree; R is the gas constant (8.31 J K^{-1} mol^{-1}); Q is the activation energy

Hence $-\dfrac{Q}{R} = -3257.3$ and

$Q = 27068$ J $= 27$ kJ

From these results, it can be concluded that the reaction between molten aluminum and Na_2SiF_6 is a controlled chemical reaction [20].
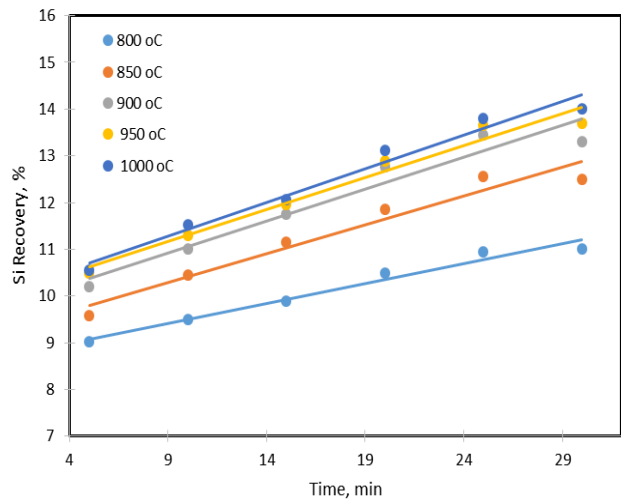

Fig. 3. The relation between the Si percentage in the produced aluminium–silicon alloys and the reaction time
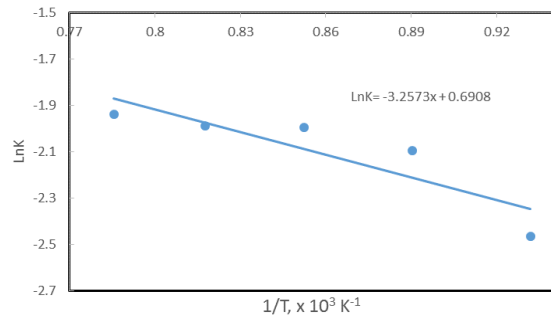

**Fig. 4.** Arrhenius plot between $\ln K$ and $1/T$

From the above results, the reaction between sodium fluosilicate with molten aluminium is taken place as follows:

- In molten aluminium, sodium fluosilicate decomposes to silicon tetra-fluoride and sodium fluoride

$$Na_2SiF_6 \rightarrow 2NaF + SiF_4(gas).\qquad(4)$$

- From thermodynamic data, the Gib's free energy for the decomposition reaction of Na_2SiF_6 is $\Delta G = 35080 - 42.51\,T$ Cal/mol
- The decomposition temperature can be obtained when $\Delta G = 0$, then T decomp $= 825.22\ K = 552.22$ °C

This temperature was close to the temperature of endothermic peak that occurs at 568 as shown in Fig. 5. It represents the DTA for Al + Na$_2$SiF$_6$ mixtures. From this figure, it could be seen that an endothermic peak at 563.26 °C represents the decomposition of Na$_2$SiF$_6$ to obtain sodium fluoride NaF and silicon tetrafluoride SiF$_4$ that being adsorbed on the surface of aluminum powder according to Eq. 4. While the endothermic peak at 659.96 °C is the latent heat of fusion for aluminum, (melting point of Al at 660 °C). The other exothermic peak, about 841.42 °C Fig. 5 might be for Al and Na$_2$SiF$_6$ to obtain Al-Si alloy with AlF$_3$ according to Eq. 5:

$$6NaF + 3SiF_4 + 4Al \rightarrow 2Na_3AlF_6 + 2AlF_3 + 3Si \text{ (alloy). (5)}$$
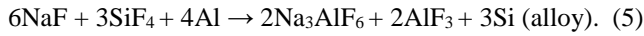
G = -149 Kcal at 841.42 and the negative sign make the reaction possible or spontaneous.
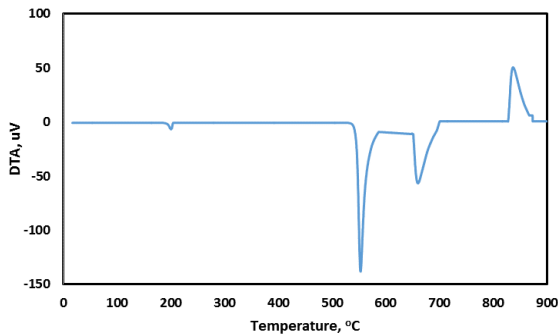

Fig. 5. DTA for Al + Na$_2$SiF$_6$ mixtures

The SiF$_4$ makes small bubbles surrounded by Si enriched layer, as shown in Fig. 6, which in turn transfers into molten aluminum by diffusion producing Al-Si alloy. While increasing the bath height may lead to increasing the contact time between molten aluminum and the bubbles bearing Si.

From the above results, it can be established that the rate of dissolution of Si in molten aluminum is chiefly governed either by the rate of Si formation or by the rate of diffusion of Si into molten aluminum. The obtained experimental data from Fig. 5 proved that the rate of Si formation proceeds according to Eq. 5.

On the other hand, as shown in Fig. 5, the diffusion of [Si] on the SiF$_4$ bubble from the boundary layer into molten Al plays a major role in forming Al-Si and it could be the rate-controlling step.

The changing rate in concentration of B in the boundary layer [B]$_o$ and boron concentration within the molten aluminium [B]$_x$ can be explained according to the following relation:

$$\frac{d[Si]_X}{dt} = k[(Si)_O - (Si)_X], \tag{6}$$

where K is the factor of proportionality, which in turn is a function of the diffusion coefficient of Si in Al [20]. I.e. the reaction velocity is proportional to the instantaneous concentration. Integrating Eq. 6 with respect to time t:

$$kt = \ln \frac{[Si]_o}{\{[Si]_o - [Si]_x\}}, \tag{7}$$

where [Si]$_o$ is the theoretical concentration of Si in the bath, i.e. all Si in SiF$_4$ could be converted into Si in the alloy; [Si]$_x$ is the concentration of Si in the produced alloy after a period of time t.

As expected, the mixing process may affect the mass transfer of Si to molten Al. In the form of Eq. 8, using the measured concentration values at different times is useful for determining the K value of reaction. From the above results, it can be concluded that the diffusion of Si from the boundary layer of the SiF$_4$ bubble to the bulk of the molten aluminum is a rate-controlling step. These results indicate that increasing the mixing speed and bath height increase the rate of Si recovery.
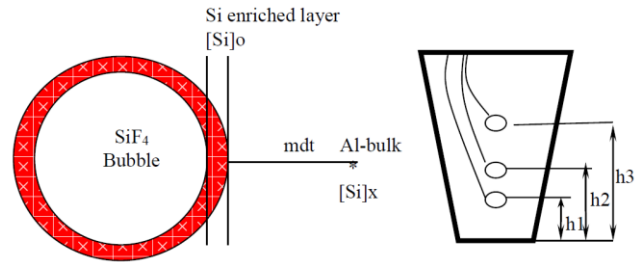

Fig. 6. Sketch for boundary layer formation

3.4. Characterization of the produced alloys

X-ray diffraction analysis (XRD) was done using Siemens D5000 diffractometer, German model using Cu radiation set at step size 0.02° and step time 0.1. The XRD pattern for Al-Si alloy containing 7 Si. Fig. 7 illustrates that there are two phases founded α Al and aluminium silicon alloy Al3.21Si0.47. The aluminium silicon alloy Al3.21Si0.47 that contains about 87.3 at % Al and 12.7 at % Si represents the eutectic composition.
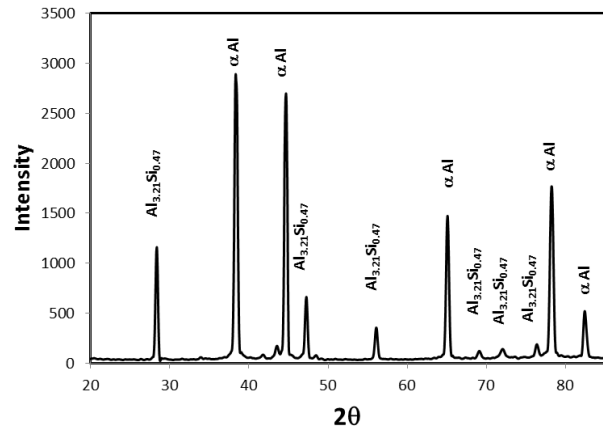

Fig. 7. XRD pattern for the produced Al-7Si alloy produced by Na$_2$SiF$_6$

Fig. 8 shows light optical microscopy (LOM) micrographs of the produced Al-Si alloys at Si contents 7 % Si modified by Na$_2$SiF$_6$. From this figure, it can be seen that a kidney shape α Al (white area) surrounded by uniformed fine fibrous eutectic Si (dark grey).

Fig. 9 shows LOM micrographs of the produced Al-Si alloys at Si content 15 % Si produced and modified by Na$_2$SiF$_6$. It can be observed that the matrix contains fibrous eutectic Si (gray color) and primary Si (black color), but the primary silicon reduces in its amount and becomes of

smaller size than the primary Si in usual (without modification) [20].

Adding sodium salts in form of Na_2SiF_6 to Al-Si alloys leads to modification of the microstructure and exchanges the point of the eutectic to a higher Si concentration.
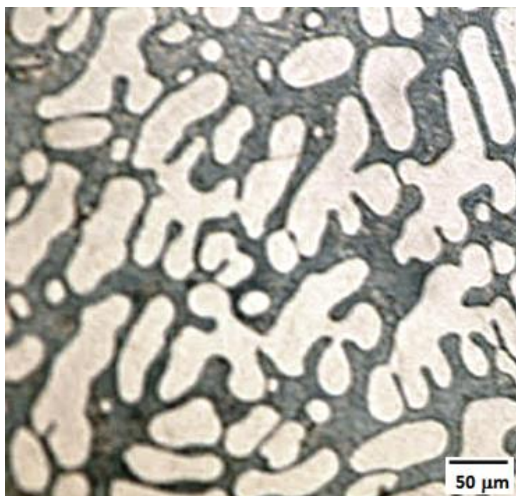

Fig. 8. LOM micrographs of the produced Al-Si alloys at Si contents 7 % Si produced by Na_2SiF_6

The aim of modifying the eutectic Si is to produce a fine fibrous form rather than the needle shape (Fig. 9). The eutectic point has shifted far enough to more than 13 % Si, at this composition, hypoeutectic instead of hypereutectic [21].
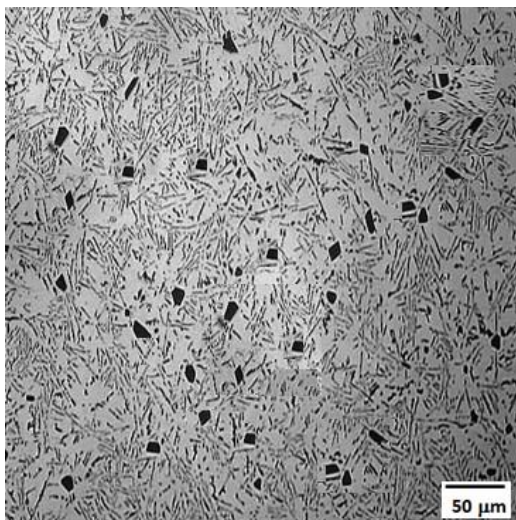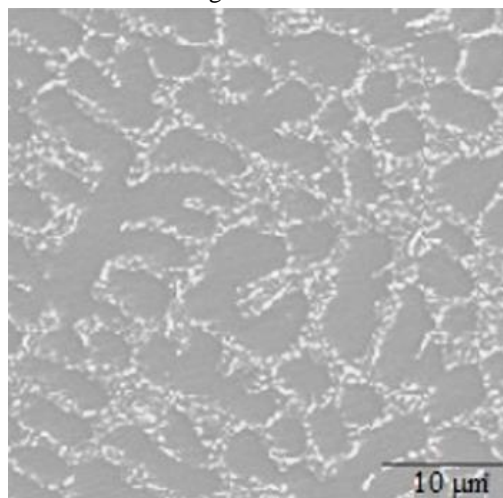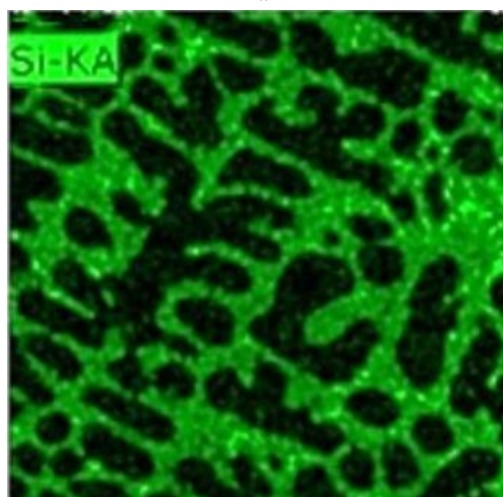

Fig. 9. LOM micrographs of the produced aluminium–silicon at Si contents 15 % Si produced by % Na_2SiF_6

Fig. 10 shows SEM and EDS mapping images of the produced aluminium–silicon alloys containing 7 % Si modified by sodium salts. The Fig. 10 a shows SEM image; the distribution of eutectic Si (lighted particle) and α Al (grey) in the matrix. It can notice that the finer fibrous in form of eutectic Si (lighted particle) around the grey area (α Al). By comparing Fig. 10 b, c to Fig. 10 a, it can be found that the fine light green color is eutectic Si around a dark color is α Al but the red color particles is α Al surrounded by eutectic silicon particles (dark color) Fig. 10 c.
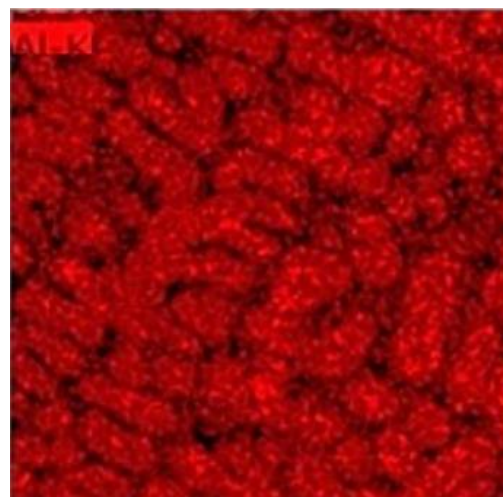
The ultimate tensile strength values (UTS) of the aluminium–silicon alloys at different percentages of Si (5, 7, 9, 11, 13 and 15 %) modified by Na_2SiF_6 salts were measured as shown in Fig. 11.

a

b

c

Fig. 10. SEM and EDS mapping images of the produced aluminium–silicon alloys containing 7 % Si modified by Na_2SiF_6 salts: a – SEM micrographs of the produced Al-Si alloys at Si contents 7% Si produced by Na_2SiF_6; b – EDS Mapping for Si particles; c – EDS Mapping for Al particles

189

It shows the effect of modification by sodium, (using Na_2SiF_6) on the UTS values of the modified Al-Si alloys. It can be observed that UTS values increase linearly by increasing the silicon contents. In addition, the hardness of the aluminium–silicon alloys at different percentages of Si (5, 7, 9, 11, 13 and 15 %) modified by Na_2SiF_6 salts increases linearly as the silicon contents increase.
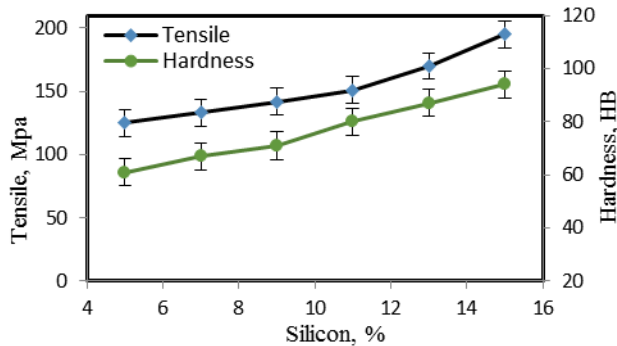

Fig. 11. Effect of Si % on the hardness and tensile strength of aluminium–silicon alloys produced by Na_2SiF_6

The wear rate of the produced specimens of Al-Si alloys that was obtained by using Na_2SiF_6, was measured at different Si contents (5, 7, 9, 11, 13 and 15 %). The wear weight loss after wear test using a pin on disk apparatus under load 0.866 kgf, sliding speed of 4.5 m/s (250 rpm) at time 7 hours, the results are indicated in Fig. 12. The wear weight loss of the produced aluminium–silicon with sodium modification reduces by increasing the Si % in the produced Al-Si alloys. The decrease of wear weight loss by increasing the percentage of silicon in the produced aluminium–silicon might be due to the existence of strengthening silicon particles that observed in the alloy [21, 22]. The wear rate as a function of Si contents could be correlated according to Eq. 8.

$$\text{wear rate, g/hr} = -0.039 \, Si \, \% + 0.606, \qquad (8)$$

where wear rate is the rate of wear loss with time at different Si contents and Si % is the needed content of silicon.
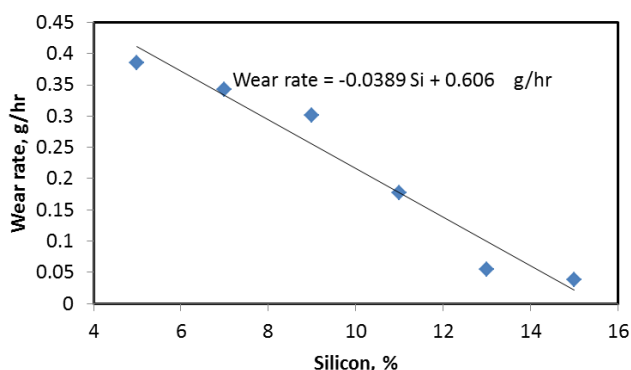

Fig. 12. Effect of Si% on the wear rate of aluminium–silicon alloys produced by Na_2SiF_6

4. CONCLUSIONS

A study was achieved to optimize the factors that affecting the preparation of a modified Al-Si alloy from the reduction of sodium fluosilicate using molten aluminium. The main conclusions are as follows:
1. The optimum conditions for producing the Al-Si alloys are; temperature 950 °C, reaction time 20 – 25 min and Na_2SiF_6/Al wt ratio depend on the Si percentage needed.
2. The prepared alloys are modified due to the presence of Na in the used material. The microstructures using LOM, SEM, and EDX indicate that the silicon shape of the hypoeutectic converted from needle to fine fibrous Si. However, at hypereutectic the primary silicon reduces in the volume fraction and size what leads to improving the morphology of all matrix.
3. The modification improves the wear and mechanical properties.

REFERENCES

1. **Stadler, F., Antrekowitsch, H., Fragner, W., Kaufmann, H., Uggowitzer, P.J.** Effect of Main Alloying Elements on Strength of Al–Si Foundry Alloys at Elevated Temperatures *International Journal of Cast Metals Research* 25 (4) 2012: pp. 215 – 224. https://doi.org/10.1179/1743133612Y.0000000004

2. **Vijeesh, V., Prabhu, K.N.** Review of Microstructure Evolution in Hypereutectic Al–Si Alloys and Its Effect on Wear Properties *Transactions of the Indian Institute of Metals* 67 (1) 2014: pp. 1 – 18. https://doi.org/10.1007/s12666-013-0327-x

3. **Sjölander, E., Seifeddine, S.** The Heat Treatment of Al–Si–Cu–Mg Casting Alloys *Journal of Materials Processing Technology* 210 (10) 2010: pp. 1249 – 1259. https://doi.org/10.1016/j.jmatprotec.2010.03.020

4. **Asghar, Z., Requena, G., Kubel, F.** The Role of Ni and Fe Aluminides on the Elevated Temperature Strength of an AlSi12 Alloy *Materials Science and Engineering: A* 527 (21 – 22) 2010: pp. 5691 – 5698. https://doi.org/10.1016/j.msea.2010.05.033

5. **Sjölander, E., Seifeddine, S.** The Heat Treatment of Al–Si–Cu–Mg Casting Alloys *Journal of Materials Processing Technology* 210 (10) 2010: pp. 1249 – 1259. https://doi.org/10.1016/j.jmatprotec.2010.03.020

6. **Stadler, F., Antrekowitsch, H., Fragner, W., Kaufmann, H., Uggowitzer, P.J.** The Influence of Solution Treatment on the High-Temperature Strength of Al-Si Foundry Alloys with Ni. In: Suarez C.E. (eds) Light Metals 2012. Springer, Cham https://doi.org/10.1007/978-3-319-48179-1_73

7. **Stadler, F., Antrekowitsch, H., Fragner, W., Kaufmann, H., Uggowitzer, P.J.** The Effect of Ni on the High-Temperature Strength of Al-Si Cast Alloys *Materials Science Forum* 690 2011: pp. 274 – 277. https://doi.org/10.4028/www.scientific.net/MSF.690.274

8. **Elmadagli, M., Perry, T., Alpas, A.T.** A Parametric Study of the relationship between microstructure and wear Resistance of Al–Si Alloys *Wear* 262 (1 – 2) 2007: pp. 79 – 92.

https://doi.org/10.1016/j.wear.2006.03.043

9. **Kim, M**. Electron Back Scattering Diffraction (EBSD) Analysis of Hypereutectic Al-Si Alloys Modified by Sr and Sc *Metals and Materials International* 13 (2) 2007: pp. 103 – 107.
https://doi.org/10.1007/BF03027559

10. **Mahato, A., Xia, S., Perry, T., Sachdev, A. Biswas, S.K.** Role of Silicon in Resisting Subsurface Plastic Deformation in Tribology of Aluminium–Silicon Alloys *Tribology International* 43 (1 – 2) 2010: pp. 381 – 387.
https://doi.org/10.1016/j.triboint.2009.06.020

11. **Nayak, S., Karthik, A.** Synthesis of Al-Si Alloys and Study of Their Mechanical Properties *A Thesis Submitted for the award of B.Sc., National Institute of Technology*, Rourkela, India, 2011.
http://ethesis.nitrkl.ac.in/2136/1/107MM004-107MM036.pdf

12. **Zhongwei, C., Zhang, R.** Effect of Strontium on Primary Dendrite and Eutectic Temperature of A357 Aluminium Alloy *China Foundry Journal* 7 (2) 2010: pp. 149 – 152.

13. **Sigworth, G.** The Modification of Al-Si Casting Alloys: Important Practical and Theoretical Aspects *International Journal of Metal casting* 2 (2) 2008: pp. 19 – 40.
https://doi.org/10.1007/BF03355425

14. **Jiang, Q., Xu, C., Wang, H, Wang, J. Yang, Y.** Estimation of the Shifting Distance of the Eutectic Point in Hypereutectic Al–Si Alloys by the Lever Rule *Scripta Materialia* 56 (5) 2007: pp. 329 – 332.
https://doi.org/10.1016/j.scriptamat.2006.11.023

15. **Nowak, M., Hari Babu, N.** Novel Grain Refiner for Hypo and Hypereutectic Al-Si Alloys *Materials Science Forum* 690 2011: pp. 49 – 52.
https://doi.org/10.4028/www.scientific.net/MSF.690.49

16. **Kanble, A.** Grain Refiners and Modifiers for the Aluminum foundry, 36 June 2014, Metal world.
http://metalworld.co.in/newsletter/2014/Jun14/Technology0614.pdf

17. **Mallapur, D., Raudupa, K., Kori, S.** Influence of Grain refiner and modifier on the microstructure and mechanical Properties A356 Alloy *International Journal of Engineering Science and Technology* 2 (9) 2010: pp. 4487 – 4493.
http://www.ijest.info/docs/IJEST10-02-09-33.pdf

18. **Ebrahim, E., Aly, I., Nofal, A. Ahmed, F., Omran, A.** Preparation of Al-Si Alloys Using Sodium – Fluosilicate and Molten Aluminium *Metall* 52 (12) 1998: pp. 712 – 715.

19. **Aly, I., Ebrahiem, E., Noval, A., Omran, A.** Dissolution Kinetics of Silicon-Containing Sodium Fluosilicate in Stirred Bath of Molten Aluminium *Annual meeting; 131st, The Minerals, Metals & Materials Society; Light metals 2002,* proceedings of the technical sessions presented by the TMS Aluminum Committee at the 131st TMA Annual Meeting; 2002; Seattle, WA.

20. **Gong, C., Tu, H., Wu, C., Wang, J., Su, X.** Study on Microstructure and Mechanical Properties of Hypereutectic Al–18Si Alloy Modified with Al–3B *Materials* 11 (3) 2018: pp. 456 – 465.
https://doi.org/10.3390/ma11030456

21. **Fredriksson, H., Akerlind, U.** Materials Processing During Casting, John Wiley & Sons Ltd, Chichester, 2006.
https://onlinelibrary.wiley.com/doi/book/10.1002/9780470017920

22. **Wang, S., Ya Liu, Y., Peng, H., Lu, X., Wang, J., Su, X.** Microstructure and Mechanical Properties of Al–12.6Si Eutectic Alloy Modified with Al–5Ti Master Alloy *Advanced Engineering Materials* 19 (12) 2017: pp. 1 – 5.
https://doi.org/10.1002/adem.201700495